J. Fluid Mech. (1979), *vol.* 91, *part* 1, *pp.* 65–91
Printed in Great Britain

The application of turbulence theory to the formulation of subgrid modelling procedures

By D. C. LESLIE
Department of Nuclear Engineering, Queen Mary College, London
AND G. L. QUARINI
H.T.F.S., Atomic Energy Research Establishment, Harwell, Oxfordshire

(Received 18 February 1977)

The problem of subgrid modelling, that is, of representing energy transfers from large to small eddies in terms of the large eddies only, must arise in any large eddy simulation, whether the equations of motion are open or direct (unaveraged) or closed (averaged). Models for closed calculations are derived from classical closures, and these are used to determine the effect of filter shape, grid-scale spectrum and grid-scale anisotropy on the effective eddy viscosity: the Leonard or resolvable-scale stress is calculated separately and is found to account for 14% of the total drain in a typical high Reynolds number case.

The validity of using these eddy viscosities in an open calculation is considered. It is concluded that this is not unreasonable, but that the simulation would be much improved if the gross drain could be separated into net drain and backscatter.

1. Introduction

Computer simulation is now well established as a valuable adjunct to experiment for the study of turbulent flows. It can provide the sort of detail which is not easily obtained from experiment, and in particular it can furnish information on the pressure fluctuations. At low Reynolds numbers ($Re_\lambda < 50$) it is possible to simulate the whole of a homogeneous turbulent field (Orszag & Patterson 1972) but this is not now possible for any real flow field or for homogeneous turbulence at high Re_λ: the range of eddy sizes outruns the speed and storage capacity of both existing and projected computers.

The remedy is well known. The simulation is confined to the large eddies or grid scales, and the interaction between these and the unrepresented small eddies or subgrid scales must be represented in terms of the large eddies only. This technique is known as subgrid modelling (Smagorinsky 1963; Lilly 1966, 1967; Deardorff 1970) and a particularly clear formulation, which will be followed in this paper, is given by Leonard (1974).

The drain of energy from the grid scales to the subgrid scales is represented by an eddy-viscosity term of the form

$$-\nu_n \nabla^2 \bar{u}_i, \tag{1.1}$$

where $\bar{u}_i$ represents the grid-scale component of the velocity (see §2) while the net eddy viscosity ν_n is derived from the local rate-of-strain tensor. Details are given below.

0022–1120/79/4133–5980 $02.00

A computer calculation of this type, in which the fluctuations of the turbulence are followed in detail, will be called a direct simulation (DS). This term includes both complete simulations and those in which subgrid modelling is used.

The alternative to direct simulation is the closed calculation, in which some form of closure is used to average out the fluctuations. The only type of closure which gives sufficient information for our purpose is the two-point variety, which seeks to express the limited triple correlations which appear in the second moment equation, namely

$$\langle u_i(\mathbf{x},t)\, u_j(\mathbf{x},t)\, u_m(\mathbf{x}',t')\rangle,$$

as functionals of the general pair correlation

$$\langle u_i(\mathbf{x},t)\, u_j(\mathbf{x}',t')\rangle.$$

Accounts of these closures are given by Monin & Yaglom (1975, vol. 2) and by Leslie (1973).

Kraichnan (1976) has shown, and this paper confirms, that the formulation of subgrid modelling is particularly straightforward in a closed calculation. The object of this paper is to examine the validity of inferring subgrid models for large eddy simulations (i.e. direct simulations of the large eddies only) from the classical closures, and to extend Kraichnan's work to the conditions under which these simulations are actually performed.

2. Generation of the grid-scale equations

Leonard (1974) separates the velocity field $u_i(\mathbf{x},t)$ into a grid-scale component $\overline{u}_i(\mathbf{x},t)$ and a subgrid component $u_i'(\mathbf{x},t)$ by a filtering operation

$$\overline{u}_i(\mathbf{x},t) = \int G(\mathbf{x},\mathbf{x}')\, u_i(\mathbf{x}',t)\, d\mathbf{x}', \tag{2.1}$$

$$u_i' = u_i - \overline{u}_i. \tag{2.2}$$

The filter G is constant in time and is normally a scalar. The overbar always denotes the filtering operation, a statistical average being indicated by angular brackets.

If the physical properties of the fluid are constant, the result of filtering the Navier–Stokes equation is

$$\frac{\partial \overline{u}_i}{\partial t} = -\frac{1}{\rho}\frac{\partial \overline{p}}{\partial x_i} - \frac{\partial R_{ij}}{\partial x_j} + \nu\nabla^2\overline{u}_i, \tag{2.3}$$

where

$$R_{ij} = \overline{\overline{u}_i\overline{u}_j + \overline{u}_i u_j' + u_i'\overline{u}_j + u_i' u_j'}. \tag{2.4}$$

The first term in R_{ij}, namely $\overline{\overline{u}_i\overline{u}_j}$, is apparently a grid-scale component, but it cannot be represented exactly as a simple functional of $\overline{u}_i$. Leonard therefore rewrites (2.3) as

$$\frac{\partial \overline{u}_i}{\partial t} = -\frac{1}{\rho}\frac{\partial \overline{p}}{\partial x_i} - \frac{\partial}{\partial x_j}\{\overline{u}_i\overline{u}_j + L_{ij} + T_{ij}\} + \nu\nabla^2\overline{u}_i. \tag{2.5}$$

$\overline{u}_i\overline{u}_j$ is the true grid-scale inertial term while

$$L_{ij} = \overline{\overline{u}_i\overline{u}_j} - \overline{u}_i\overline{u}_j \tag{2.6}$$

is now known as the Leonard stress. Finally

$$T_{ij} = \overline{\overline{u}_i u_j' + u_i'\overline{u}_j + u_i' u_j'} \tag{2.7}$$

is the true subgrid stress. It measures the effect of the unrepresented subgrid scales on the evolution of the grid scales. Leonard approximates L_{ij} by

$$L_{ij} = G_2 \nabla^2(\bar{u}_i \bar{u}_j), \tag{2.8}$$

where

$$G_2 = \int \tfrac{1}{6}\xi^2 G(\boldsymbol{\xi})\, d^3\boldsymbol{\xi} \tag{2.9}$$

is the (spherical) second moment of the filter.

Any finite-difference scheme will filter the raw velocity components u_i, but Kwak, Reynolds & Ferziger (1975) find that the simulation is improved if the Navier–Stokes equations are prefiltered before the finite-difference scheme is applied. For best results the filter should have about twice the width of the finite-difference mesh: a Gaussian shape is suitable and convenient. Love (1978, private communication) has shown that these findings are also valid for the Burgers equation.

2.1. *The subgrid model*

All subsequent workers have followed Smagorinsky (1963) and have represented the true subgrid drain T_{ij} by an eddy-viscosity model†

$$T_{ij} = -\nu_n \left(\frac{\partial \bar{u}_i}{\partial x_j} + \frac{\partial \bar{u}_j}{\partial x_i}\right) \tag{2.10}$$

so that the complete grid-scale equation reads

$$\frac{\partial \bar{u}_i}{\partial t} = -\frac{1}{\rho}\frac{\partial \bar{p}}{\partial x_i} - \frac{\partial}{\partial x_j}\{\bar{u}_i \bar{u}_j + G_2 \nabla^2(\bar{u}_i \bar{u}_j)\} + \frac{\partial}{\partial x_j}\left\{(\nu + \nu_n)\left(\frac{\partial \bar{u}_i}{\partial x_j} + \frac{\partial \bar{u}_j}{\partial x_i}\right)\right\}. \tag{2.11}$$

If ν_n is independent of $\mathbf{x}$, the last term reduces to $(\nu + \nu_n)\nabla^2 u_i$.

The net eddy viscosity ν_n will depend on the filter width h and on ϵ, the total rate of dissipation of energy in the subgrid scales. If ν_n is determined by these two variables only, then dimensional analysis gives

$$\nu_n = F \epsilon^{\frac{1}{3}} h^{\frac{4}{3}}. \tag{2.12}$$

It will be shown later that the non-dimensional constant F depends on the nature of the filter and on the spectrum of the large (grid-scale) eddies.

It is not easy to estimate ϵ in a large eddy simulation and Smagorinsky therefore replaced (2.12) by

$$\nu_n = c^2 h^2 \bar{S}^{\frac{1}{2}}, \tag{2.13}$$

where

$$\bar{S} = \frac{\partial \bar{u}_i}{\partial x_j}\left(\frac{\partial \bar{u}_i}{\partial x_j} + \frac{\partial \bar{u}_j}{\partial x_i}\right) \tag{2.14}$$

is related to the grid-scale deformation tensor, while c is another non-dimensional constant. (In §4 we show that (2.12) and (2.13) are compatible, and deduce the relation between c and F.) Some workers (see, for example, Kwak *et al.* 1975) have preferred to use the grid-scale vorticity $\bar{\Omega}$ rather than $\bar{S}$. The two quantities are equivalent in the homogeneous isotropic flows with which this paper is mainly concerned.

In his highly successful simulation of channel flows Schumann (1973, 1975) related ν_n to the subgrid energy $\bar{E}'$ rather than to $\bar{S}$. In essence his model is

$$\nu_n = c_2 h (\bar{E}')^{\frac{1}{2}}$$

† Until Leonard (1974) pointed out the special character of the Leonard stress, this representation was applied to the total stress $L_{ij} + T_{ij}$. We refer to this point later.

though its practical implementation in a finite-difference scheme is more complex than this. $\bar{E}'$ is determined by solving a balance equation derived from the subgrid component of the Navier–Stokes equations: the source in this equation is the drain from the grid scales. This approach is radically different from Smagorinsky's and we do not attempt to analyse it in this paper.

2.2. *The filters*

For reasons explained in § 3.1, the flow will be supposed to be homogeneous. The filter $G(\mathbf{x}, \mathbf{x}')$ then simplifies to a difference function $G(\mathbf{x}-\mathbf{x}')$, and (2.1) has the Fourier transform

$$\bar{u}_i(\mathbf{k}, t) = G(\mathbf{k})\, u_i(\mathbf{k}, t). \tag{2.15}$$

Three filters have been considered. The simplest is the spherically symmetric sharp filter (the 'subgrid-scale filter' of Kwak *et al.* 1975)

$$G(k) = \begin{cases} 1 & \text{if} \quad k < K_1, \\ 0 & \text{if} \quad k > K_1. \end{cases} \tag{2.16}$$

(The underlining indicates the short title which identifies the filter.) The Gaussian filter

$$G(k) = \exp\left(-\tfrac{1}{24} k^2 h^2\right) \tag{2.17}$$

is also symmetric, while the top-hat filter

$$G(\mathbf{x}-\mathbf{x}') = \begin{cases} h^{-3} & \text{if} \quad |x_i - x_i'| < \tfrac{1}{2}h \quad (i = 1, 2, 3), \\ 0 & \text{otherwise} \end{cases} \tag{2.18}$$

is weakly anisotropic. This filter is of some practical interest, since it is generated by a second-order central-difference scheme in which the finite-difference mesh is moved over the velocity field, rather than being fixed in space: so long as the field is homogeneous, this movement does not affect the results.

The Fourier transform of (2.18) is

$$G(k) = B(\tfrac{1}{2}k_1 h)\, B(\tfrac{1}{2}k_2 h)\, B(\tfrac{1}{2}k_3 h), \tag{2.19}$$

where

$$B(v) = \sin v / v,$$

and the calculations reported below are made on the isotropic component of this filter

$$G_0(k) = \frac{1}{4\pi} \oint G(\mathbf{k})\, d\Omega_k. \tag{2.20}$$

We have shown, by spherical harmonic expansion, that the resulting error is proportional to the square of the relative anisotropy, and that it is negligible for this filter.† These two filters prove to be rather similar, and we emphasize the Gaussian because a 'real-life' large eddy simulation will be dominated by the Gaussian prefilter, whose (wavenumber) width will be about half that of the filter of top-hat type implied by the finite-difference scheme.

† This work has been omitted to save space. Details are available from the authors on request.

Two filters are equivalent for this purpose if they have the same value of G_2 [see (2.9)] and the Gaussian (2.17) is equivalent to the top-hat filter (2.18) in this sense, both having $G_2 = \frac{1}{24}h^2$. However the integral G_2 does not exist for the sharp filter (2.16) and we therefore prefer to define equivalence as implying the equality of the width

$$W = \int_0^\infty G_0(k)\,dk. \tag{2.21}$$

On this basis the sharp filter is equivalent to the top-hat filter if

$$K_1 = 2{\cdot}957h^{-1} \tag{2.22}$$

and we redefine the Gaussian as

$$G(k) = \exp\left(-\frac{k^2h^2}{22{\cdot}27}\right) \tag{2.23}$$

so that it has the same width. The comparisons reported below are all on this basis.

3. Subgrid modelling in a closed calculation

At a Reynolds number of 10^6, the largest eddies in a turbulent flow are roughly 1000 times bigger than the dissipation eddies. A full (three-dimensional) direct simulation would require upwards of 10^9 mesh points and a very small time step. This fact led Corrsin (1961) to conclude not only that the calculation was impractical at that time but that it would probably always be infeasible.

A similar argument applies to a closed calculation on a real flow. The calculation now has a minimum of four space dimensions (Leslie 1973, chap. 15). In each dimension fewer mesh points are required than in a direct simulation because the correlation functions are smooth while the raw (fluctuating) velocities are not, but this saving could well be more than cancelled by the increase in dimensionality. Therefore there is also a subgrid modelling problem in closed calculations.

In this section we consider how this latter problem may be tackled: in §5 we examine the implications of this work for subgrid modelling in a large eddy simulation. The analysis limited to homogeneous flows: for convenience, we shall also assume stationarity. Closures such as direct interaction can be applied to inhomogeneous flows (Kraichnan 1964) but at present the application is purely formal. If the flow is homogeneous, the various tensors are diagonal in a wavenumber representation. No diagonalizing representation is known for any inhomogeneous flow, and without this simplification it has proved impossible to extract practical results from the equations. In §5 it will be argued that this limitation is not as serious as it seems.

3.1. *Subgrid modelling in a homogeneous isotropic flow*

Transforming to wavenumber space and eliminating the pressure, the equation of motion reads

$$\left(\frac{d}{dt}+\nu k^2\right) u_i(\mathbf{k},t) = M_{ijm}(\mathbf{k}) \overset{\Delta}{\sum} u_j(\mathbf{p},t)\, u_m(\mathbf{r},t) + F_i(\mathbf{k},t), \tag{3.1}$$

where

$$M_{ijm}(\mathbf{k}) = -\frac{i}{2}\left[k_m P_{ij}(\mathbf{k}) + k_j P_{im}(\mathbf{k})\right],$$

$$P_{ij}(\mathbf{k}) = \delta_{ij} - \frac{k_i k_j}{k^2}$$

and

$$\overset{\Delta}{\sum} \text{implies} \iint \delta(\mathbf{k}-\mathbf{p}-\mathbf{r})\, d^3\mathbf{p}\, d^3\mathbf{r}$$

(Leslie 1973). In (3.1), $F_i(\mathbf{k})$ represents the driving force which sustains the turbulence. In a large eddy simulation this force will be represented explicitly: it seems that it will play no part in transferring energy from the large eddies to the small ones.

Unless the whole of the flow is homogeneous the grid-scale pressure cannot be eliminated algebraically, as it has been from (3.1). It is standard practice in large eddy simulations to compute the pressure explicitly.

The equation of motion for the grid-scale velocity $\bar{u}_i(\mathbf{k}, t)$ is formed from (3.1) by filtering according to (2.14): it is

$$\left(\frac{d}{dt}+\nu k^2\right) \bar{u}_i(\mathbf{k}, t) = M_{ijm}(\mathbf{k}) \overset{\Delta}{\sum} G(\mathbf{k})\, u_j(\mathbf{p}, t)\, u_m(\mathbf{r}, t) + G(\mathbf{k})\, F_i(\mathbf{k}, t). \tag{3.2}$$

The inertial term on the right-hand side of (3.2) can be brought into correspondence with the analysis of Leonard (1974) by splitting it up thus:

$$M_{ijm}(\mathbf{k}) \overset{\Delta}{\sum} [\underbrace{G(\mathbf{p})\, G(\mathbf{r})}_{①} - \underbrace{\{1-G(\mathbf{k})\}\, G(\mathbf{p})\, G(\mathbf{r})}_{②}$$
$$+ \underbrace{G(\mathbf{k})[G(\mathbf{p})\{1-G(\mathbf{r})\} + G(\mathbf{r})\{1-G(\mathbf{p})\} + \{1-G(\mathbf{p})\}\{1-G(\mathbf{r})\}]}_{③}]\, u_j(\mathbf{p}, t)\, u_m(\mathbf{r}, t). \tag{3.3}$$

Term ① is $\bar{u}_j \bar{u}_m$; being represented explicitly in the large eddy simulation, it does not contribute to the subgrid stresses.

Term ② is the resolvable-scale or Leonard stress L_{ij} [see (2.6)].

Term ③ is the true subgrid stress T_{ij} [see (2.7)] and can be collapsed to

$$\overset{\Delta}{\sum} G(\mathbf{k})\{1-G(\mathbf{p})\, G(\mathbf{r})\}\, M_{ijm}(\mathbf{k})\, u_j(\mathbf{p})\, u_m(\mathbf{r}). \tag{3.4}$$

The object of subgrid modelling is to represent this term as a functional of $\bar{u}$.†

The classical closures work, not with primitive equations such as (3.3), but with second-moment equations formed from them. In particular the grid-scale energy

$$\bar{E}(k, t) = \tfrac{1}{2} k^2 \oint \langle \bar{u}_i(\mathbf{k}, t)\, \bar{u}_i(-\mathbf{k}, t) \rangle\, d\Omega_k \tag{3.5}$$

is related to the total scalar energy $E(k, t)$ by

$$\bar{E}(k, t) = G^2(k)\, E(k, t). \tag{3.6}$$

The inertial contribution to the equation of motion for $\bar{E}$ is formed from (3.3) according to

$$\oint k^2 d\Omega_k \langle G(k)\, u_i(-\mathbf{k}, t)\, \{\text{form (3.3)}\} \rangle. \tag{3.7}$$

(The factor $\frac{1}{2}$ in (3.5) cancels since we are working on the time diagonal.) The final equation is

$$(d/dt + \nu k^2)\, \bar{E}(k, t) = \text{grid-scale inertial transfer} + \text{Leonard term} + \text{true subgrid term} + \text{forcing term}, \tag{3.8}$$

† There is no need for such modelling in a closed calculation on a homogeneous isotropic flow, since the functions are then one-dimensional and can be represented in full. However, the work does show rather simply how such modelling can be effected.

where

$$\text{Leonard term} = -\tfrac{1}{2}\iint^{\Delta} dp\,dr G(k)\{1-G(k)\}G(p)G(r)S(k|pr) \tag{3.9}$$

and

$$\text{true subgrid term} = \tfrac{1}{2}\iint^{\Delta} dp\,dr G^2(k)\{1-G(p)G(r)\}S(k|pr). \tag{3.10}$$

Here

$$S(k|pr) = 16\pi^2 kpr M_{ijm}(\mathbf{k})\langle u_j(\mathbf{p})u_m(\mathbf{r})u_i(-\mathbf{k})\rangle. \tag{3.11}$$

(Strictly, $S(k|pr)$ is the isotropic part of the quantity on the right side: the anisotropic parts vanish when the angular integration described in the appendix is performed.) The double integral is over the region

$$|k-p| < r < k+p, \tag{3.12}$$

in which $\mathbf{p}$ and $\mathbf{r}$ can form a triangle with $\mathbf{k}$ (Leslie 1973).

The aim of this section is to derive subgrid models by using the functional relationship which the classical closures give between $S(k|p,r)$ and second moments such as E. Provided that the response and correlation functions are assumed to have the same exponential dependence on time

$$\left.\begin{aligned} G^{(\mathrm{res})}(k,\tau) &= \exp\{-\eta(k)\tau\}, \quad \tau > 0, \\ R(k,\tau) &= \exp\{-\eta(k)|\tau|\} \end{aligned}\right\} \tag{3.13}$$

(see Leslie 1973 for a discussion of this assumption and of the formulae given below) then all the classical closures now available give the same functional form for the inertial transfer function $S(k|p,r)$ on the main time diagonal $t' = t$. This is

$$\begin{aligned} S(k|p,r) = [\eta(k)+\eta(p)+\eta(r)]^{-1}[&B(k,p,r)q(r)\{q(p)-q(k)\} \\ &+ B(k,r,p)q(p)\{q(r)-q(k)\}], \end{aligned} \tag{3.14}$$

where

$$q(k) = E(k)/4\pi k^2,$$

$$B(k,p,r) = 16\pi^2 k^3 prb(k,p,r), \quad b(k,p,r) = (p/k)(xy+z^3),$$

x, y and z being the cosines of the angles opposite $\mathbf{k}$, $\mathbf{p}$ and $\mathbf{r}$ in the triangle formed by these vectors, while η is defined by (3.11). In this equation, the response function is called $G^{(\mathrm{res})}$ to distinguish it from the filter function $G(k)$.

Combining (3.11) and (3.14), the true subgrid drain can be put into the form

$$\text{true subgrid drain} = 2k^2\nu_d(k)E(k) - U(k), \tag{3.15}$$

where

$$\nu_d(k) = \sum^{\Delta} \frac{rb(k,p,r)E(r)}{2kp[\eta(k)+\eta(p)+\eta(r)]}[1-G(p)G(r)], \tag{3.16}$$

$$U(k) = \sum^{\Delta} \frac{k^3 b(k,p,r)E(p)E(r)}{pr[\eta(k)+\eta(p)+\eta(r)]}G^2(k)[1-G(p)G(r)]. \tag{3.17}$$

In Leonard's formalism, the standard eddy-viscosity assumption implies that

$$\text{true net subgrid drain} = 2k^2\nu_n\bar{E}(k) \tag{3.18}$$

and (3.15) shows that the classical closures do not wholly support this form. Rather, these closures indicate that the gross drain is proportional to the local excitation, and that this gross drain is partly offset by a return of energy from the subgrid scales.

This is just as one would expect and the fact that the classical closures produce this result quite naturally is one of the strongest reasons for thinking that they may be broadly correct.

Equation (2.12) implies that ν_n depends only on the gross properties of the local turbulence and that it is independent of the details of the spectrum. Equations (3.16) and (3.17) show that this is roughly true of $\nu_d(k)$ and $U(k)$. $E(p)$ and $E(r)$ may be assumed to have the universal inertial-range form, and the effect of the functional dependence of $\eta(k)$ on $\bar{E}(k)$ will be small since $\eta(k)$ will be smaller than $\eta(p)$ and $\eta(r)$. However if (3.15) is forced into the form (3.18), then

$$\nu_n(k) = \nu_d(k) - U(k)/2k^2\bar{E}(k) \tag{3.19}$$

and this must be sensitive to the form of $\bar{E}$. In large eddy simulations ν_n is assumed to be independent of k, and the accuracy of this assumption is tested below by calculation.

In this closed calculation the Leonard drain term is

$$-2\left\langle \overline{u}_i \frac{\partial}{\partial x_j}(\overline{\overline{u}_i \overline{u}_j} - \overline{u}_i \overline{u}_j) \right\rangle$$

[see (2.5) and (2.6)] and (3.9) is the Fourier transform of this quantity. We could treat it as we treated the true drain term, but this would not be faithful to actual large eddy simulations, where the term is modelled according to Leonard's approximation (2.8). The equivalent of this approximation in a closed calculation is

$$-2G_2\langle \overline{u}_i \partial^3 \overline{u}_i \overline{u}_j / \partial x_j \partial x_m \partial x_m \rangle \tag{3.20}$$

and the Fourier transform of this quantity is

$$-\tfrac{1}{2}\iint^{\Delta} dp\, dr G_2 k^2 G(k)\, G(p)\, G(r)\, S(k|pr). \tag{3.21}$$

Evidently, Leonard is approximating the factor $1 - G(k)$ in (3.9) by $G_2 k^2$. Below, we compare results derived from the approximate form (3.21) with those given by the exact form (3.9).

3.1.1. *The sharp filter with inertial-range spectra.* The formulae simplify somewhat if the filter is sharp, and in particular the Leonard stress is identically zero. k will be in the grid-scale range $k < K_1$ [see (2.16)] and both $\nu_d(k)$ and $U(k)$ will be zero unless p and/or r are in the subgrid range $p, r > K_1$. The formulae for ν_d and U simplify to

$$\nu_d(k) = \iint^{\Delta}_{p \text{ or } r > K_1} dp\, dr\, \frac{rb(k,p,r)\, E(p)}{2pk[\eta(k) + \eta(p) + \eta(r)]} \tag{3.22}$$

and

$$U(k) = \iint^{\Delta}_{p \text{ or } r > K_1} dp\, dr\, \frac{k^3}{pr}\, \frac{b(k,p,r)\, E(p)\, E(r)}{\eta(k) + \eta(p) + \eta(r)}. \tag{3.23}$$

The region of integration, which is now further restricted by the requirement that p or r should be greater than K_1, is shown in figure 1.

Equations (3.22) and (3.23) simplify further when $E(k)$ and $\eta(k)$ have the inertial-range forms

$$E(k) = K o \epsilon^{\frac{2}{3}} k^{-\frac{5}{3}}, \quad \eta(k) = D \epsilon^{\frac{1}{3}} k^{\frac{2}{3}}. \tag{3.24}$$

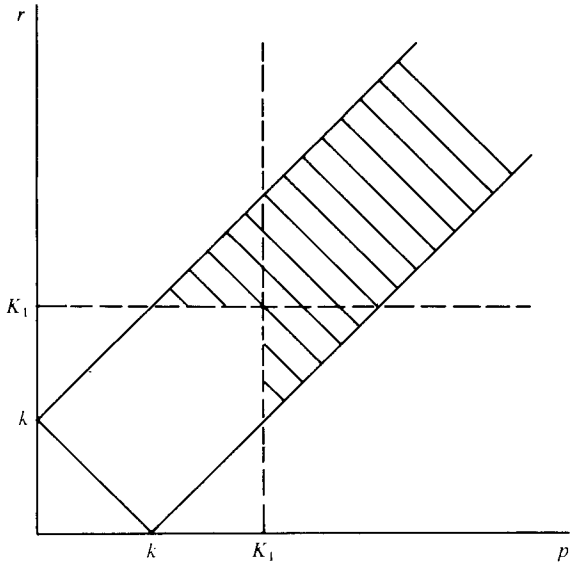

FIGURE 1. Region of integration for the sharp filter.

Here ϵ is the total rate of dissipation of turbulent energy, and Ko is the Kolmogorov constant. The value

$$Ko = 1{\cdot}5, \tag{3.25}$$

which is reasonably representative of experimental data, will be used throughout this paper. Kraichnan (1971) has shown that use of the form (3.14) for $S(k|p,r)$ implies

$$D/Ko^2 = 0{\cdot}1904 \tag{3.26}$$

and it is therefore consistent to put

$$D = 0{\cdot}1904 \times (1{\cdot}5)^2 = 0{\cdot}4284. \tag{3.27}$$

This value is also used throughout. The inertial-range forms are reasonable for the subgrid range, but they are unrealistic for the grid-scale range since they imply that all the production processes are concentrated at $k = 0$ and that nothing other than inertial transfer happens at finite values of k. The results would be relevant if the grid scales extended far into the inertial range, and they are therefore interesting as the limit of a practical situation.

Kraichnan (1976) has evaluated the inertial-range forms of the integrals (3.22) and (3.23). He finds that for $k \ll K_1$ the drain part of the eddy viscosity is constant and that its value is

$$\nu_d(0) = \frac{1}{12}\frac{Ko}{D}\epsilon^{\frac{1}{3}}K_1^{-\frac{4}{3}} \tag{3.28}$$

$$= 0{\cdot}292\epsilon^{\frac{1}{3}}K_1^{-\frac{4}{3}} \tag{3.29}$$

using our preferred values of Ko and D. At these low wavenumbers the drain term $k^2\nu_d(k)E(k)$ varies as $k^{\frac{1}{3}}$, while the input or backscatter term varies as k^4 and is negligible. $\nu_d(k)$ rises steadily with increasing k, and it has an integrable divergence of the form $(K_1-k)^{-\frac{2}{3}}$ at the cut. Kraichnan remarks, and we shall confirm, that this

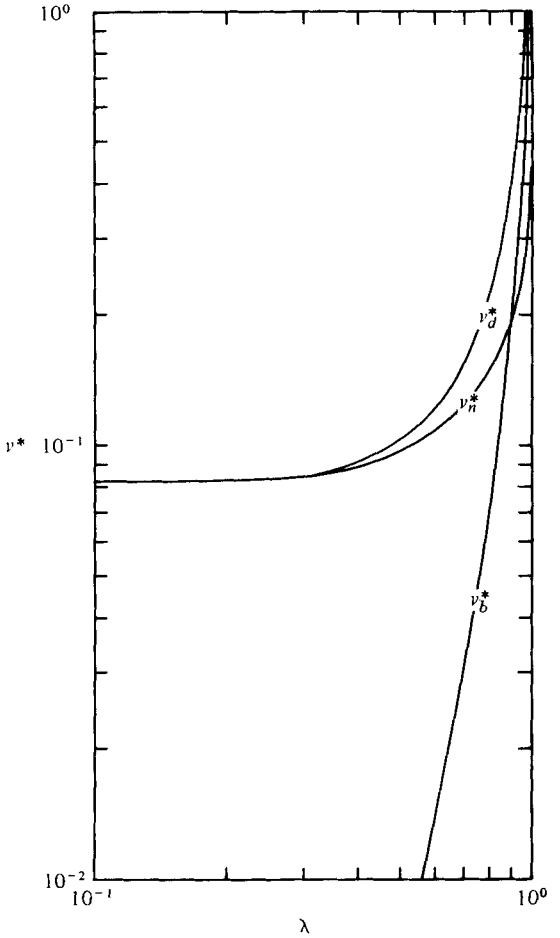

FIGURE 2. ν_d^*, ν_b^* and ν_n^* for the sharp filter.

divergence disappears if the inertial-range spectrum does not continue right down to $k = 0$.

The backscatter term rises rapidly as k approaches K_1, and at the cut it has a singularity which exactly cancels the singularity in the drain term. The net eddy viscosity defined by (3.19) is everywhere finite, and

$$\nu_n(K_1) = 5{\cdot}24\nu_d(0). \tag{3.30}$$

The dependence of ν_d, $\nu_b = U/2k^2\bar{E}(k)$ and the net drain viscosity ν_n on k is shown in figure 2. ν_b may be thought of as the 'backscatter eddy viscosity': for consistency in presentation, we plot this quantity rather than the backscatter energy $U(k)$.

We have already noted that existing large eddy simulations replace this complex k dependence by a (constant) average net eddy viscosity ν_n^{av}. This must drain energy out of the grid scales at a rate ϵ, and ν_n^{av} may therefore be found from energy balance without detailed calculation. The governing equation is

$$\int_0^{K_1} 2k^2\nu_n^{\mathrm{av}} Ko\,\epsilon^{\frac{2}{3}} k^{-\frac{5}{3}} dk = \epsilon,$$

or

$$\nu_n^{\mathrm{av}} = 0{\cdot}127\, Ko\, D^{-1}\epsilon^{\frac{1}{3}} K_1^{-\frac{4}{3}} \tag{3.31}$$

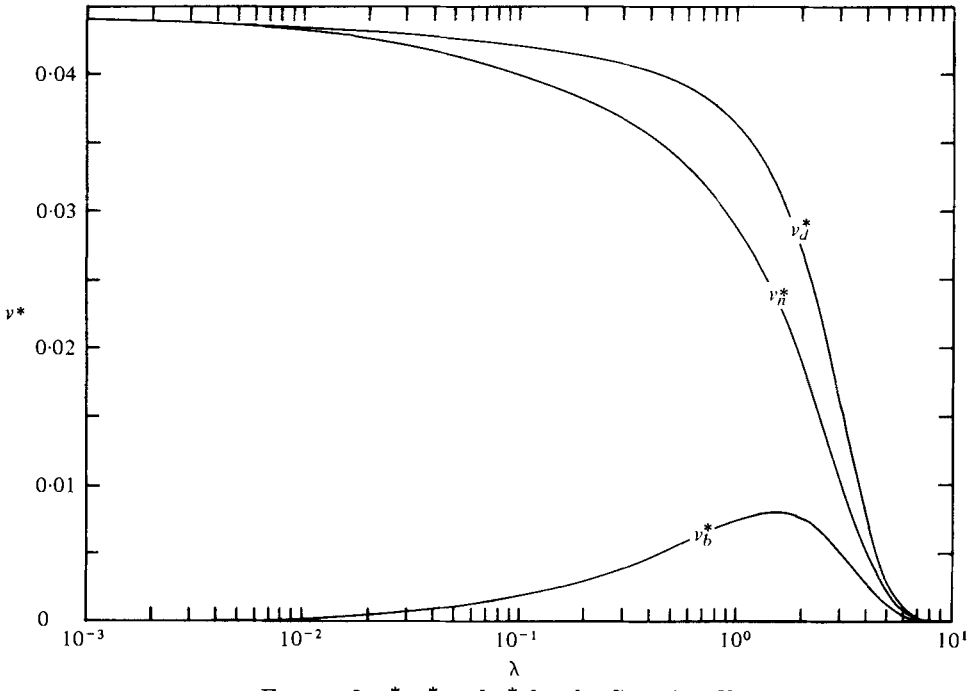

FIGURE 3. ν_d^*, ν_b^* and ν_n^* for the Gaussian filter.

since D/Ko^2 is fixed [see (3.26)]. Kraichnan found that the factor multiplying $Koc^{\frac{1}{2}}K_1^{-\frac{4}{3}}/D$ rose from 0·0833 at $k = 0$ to 0·437 at $k = K_1$, and this is compatible with (3.31). The connexion between this result and the calculation of Lilly (1966) is considered in § 4.

3.1.2. *Inertial-range spectra with graded filters.* (This term indicates a filter which falls smoothly from 1 to 0.) Figure 3 shows $\nu_d(k)$, $\nu_b(k)$ and $\nu_n(k)$ for the Gaussian filter

$$\exp(-k^2h^2/22{\cdot}26) \tag{3.32}$$

which has the same width $W = 2{\cdot}975h^{-1}$ as a top-hat filter on a mesh of spacing h (see § 2). The figure is actually a non-dimensional plot of

$$\nu^*(\lambda) = \nu(\lambda)/\{Ko\,D^{-1}\epsilon^{\frac{1}{3}}h^{\frac{4}{3}}\} \tag{3.33}$$

as a function of $\lambda = kh$. The Leonard stress is now non-zero, and it has been included in the gross drain term $\nu_d(k)$: its magnitude and behaviour are discussed below.

The contrast with the behaviour of the sharp filter, as shown in figure 2, is very marked. The drain viscosity ν_d^* is nearly constant over the grid-scale range of wavenumbers $k < 1/h$, though it drops slightly as k approaches $1/h$. (This wavenumber sets the scale of the Gaussian filter, but it is not critical in the way that the cut wavenumber K_1 is for the sharp-filter.) The backscatter viscosity ν_b^* is small for $\lambda \ll 1$, but it rises rapidly as λ approaches 1. The net viscosity ν_n^* falls steadily over the grid-scale range, its value at $\lambda = 1$ being about two-thirds of its value at $\lambda = 0$.

The Leonard drain term has also been calculated for the Gaussian filter (3.32), assuming the grid-scale spectrum to be of inertial form throughout. The exact and

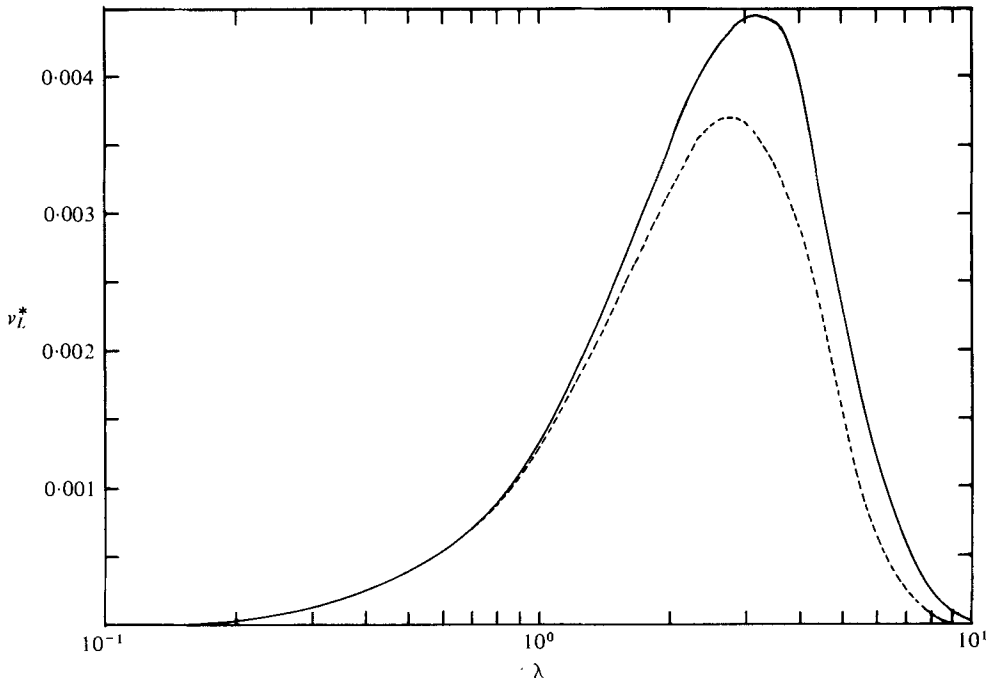

FIGURE 4. Exact and approximate Leonard viscosities ν_{Le}^* and ν_{La}^* respectively. ——, ν_{La}^*; – – –, ν_{Le}^*.

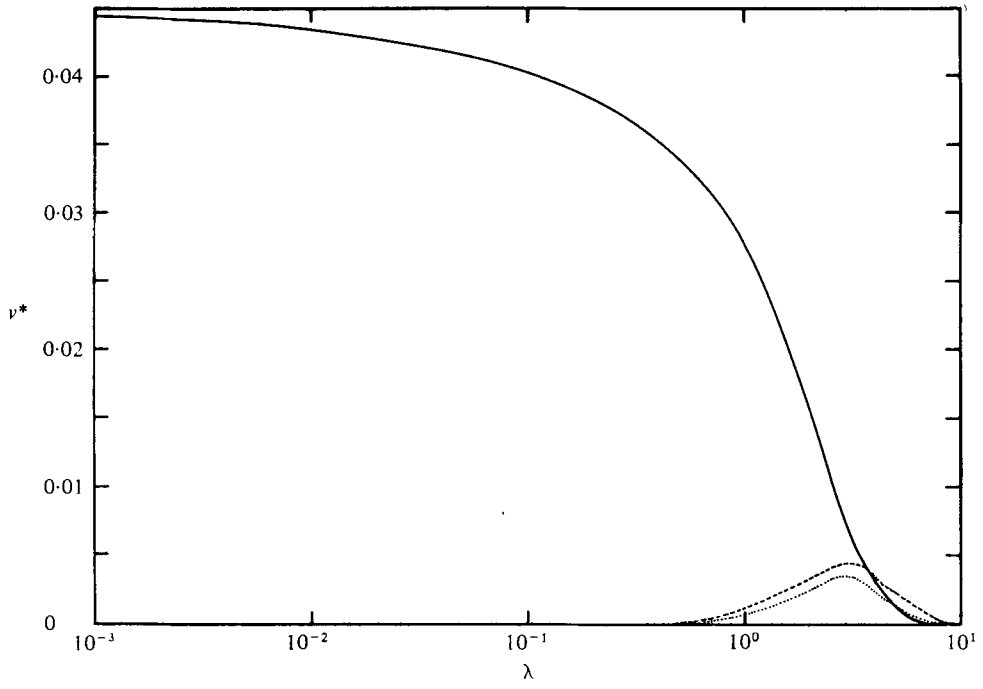

FIGURE 5. Exact and approximate Leonard viscosities compared with the total true subgrid viscosity. ——, ν_t^*; – – –, ν_{La}^*; · · · · ·, ν_{Le}^*.

approximate Leonard drain terms have been computed from (3.9) and (3.21): these terms are used to define exact and approximate Leonard viscosities according to

$$\text{right-hand side of (3.9)} = -2\nu_{Le}(k)\,k^2\bar{E}(k), \tag{3.34}$$

$$\text{right-hand side of (3.21)} = -2\nu_{La}(k)\,k^2\bar{E}(k), \tag{3.35}$$

and these are then non-dimensionalized according to (3.33). Figure 4 shows ν^*_{Le} and ν^*_{La} as functions of λ while figure 5 superimposes this information on a plot of the true net drain ν^*_t. (By definition $\nu^*_n = \nu^*_t + \nu^*_{Le}$.)

As one would expect, Leonard's approximation (2.8) [or (3.21)] overestimates the Leonard stress: in this case the approximate formulation gives 19·2% too much drain of energy from the grid scales. This is not as serious as it sounds since, as figure 5 shows, the Leonard viscosity is only a small fraction of the total drain viscosity. Since the viscosity is weighted with $k^2E(k) \propto k^{\frac{1}{3}}$ for this inertial-range spectrum, the Leonard contribution is rather greater than this graph would suggest: in this case it is responsible for 14·2% of the total drain. Thus Leonard's approximation overestimates the total gross drain by about 3%, which is very acceptable.

3.1.3. *The effect of a production-type spectrum.* In a 'real-life' large eddy simulation, the grid-scale spectrum will not have the inertial-range form $E(k) = Ko\epsilon^{\frac{2}{3}}k^{-\frac{5}{3}}$. The actual spectral intensity must be less than this, and it is generally believed that $E(0) = 0$. We shall call such a form a production-type spectrum, since it is closely related to the processes by which the turbulence extracts energy from the mean field. The large eddy simulation will determine the form of this function† and the computational mesh will be arranged as so to resolve it as well as possible.

The mesh will resolve the production eddies only. With existing and projected computers, there is no possibility of representing inertial-range eddies explicitly, and indeed it is more likely that important production events will be lost in the subgrid scales. Therefore in large eddy simulations the grid-scale spectrum cannot be wholly or even largely of inertial-range form. There is therefore a need to investigate the effect of production-type spectra on the subgrid drain.

The forms of these spectra are not known, and they must be postulated. Provided the production phenomena can be described by a single length scale, the spectrum must be of the form

$$E(k) = A_s(k/K_p)\,Ko\,\epsilon^{\frac{2}{3}}k^{-\frac{5}{3}}. \tag{3.36}$$

Here K_p is proportional to the wavenumber at which the spectrum is a maximum [and also to the width as defined by (2.21)], and A_s is a function which must tend to 1 as $k/K_p \to \infty$. There are no other strong constraints on its form. We have found it convenient to suppose that

$$A_s(z) = z^{s+\frac{5}{3}}/(1+z^{s+\frac{5}{3}}), \tag{3.37}$$

which gives $E(k) \propto k^s$ for small k.

A paper by Lesieur & Schertzer (1977) has important implications for the form of $E(k)$ when k is small. Using the eddy-damped quasi-normal Markovian (EDQNM)

† The production processes are essentially inhomogeneous, and it is not clear how far they can be represented as functions of a single vector variable in wavenumber space. This doubt can be resolved only by extending the classical closures to inhomogeneous flows: until this is done, there is no reasonable alternative to representing production processes in terms of $q(k)$.

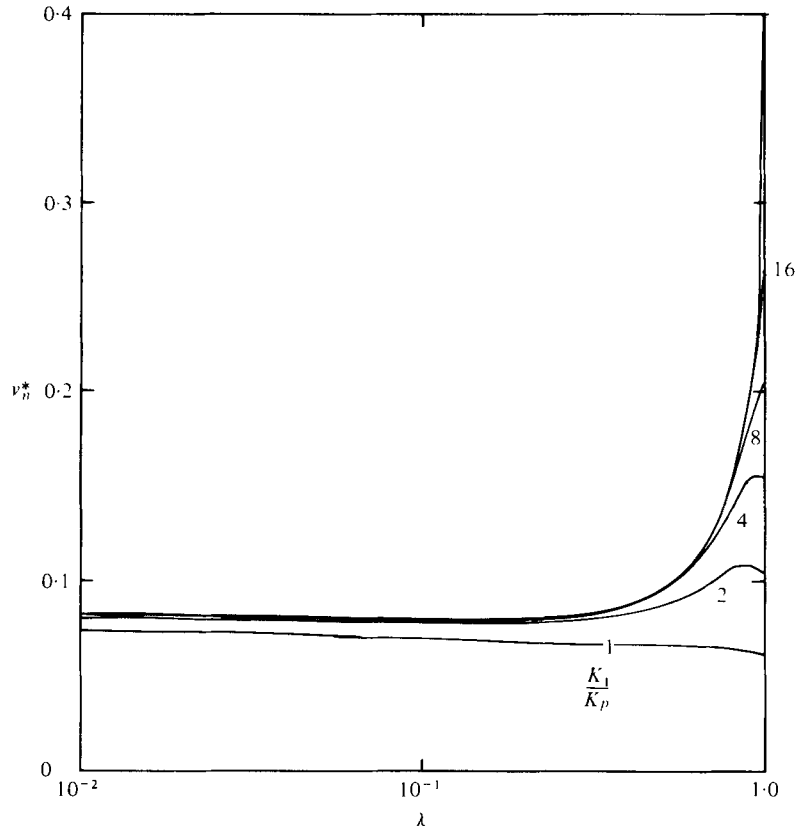

FIGURE 6. ν_n^* for the sharp filter and the A_1 production spectrum with various values of K_1/K_p.

closure of Orszag (1970) they have shown that there are self-similar inviscid solutions of the form

$$E(k,t) = t^n \Gamma(kt^m)$$

in which the longest waves are invariant over long periods of time and are of the form $k^s, s = -n/m$. s cannot be greater than 4: if it is, backscatter will immediately create a k^4 spectrum. The energy

$$E_0 = \int_0^\infty E(k)\,dk$$

decays as $t^{-2(s+1)/(s+3)}$.

For $s = 1$ ($E_0 \propto t^{-1}$) only, a self-similar solution can persist in the presence of molecular viscosity. We have therefore made most of our calculations for $s = 1$; provided s is less than 4, the results are rather insensitive to its precise value.† (As indicated above, s cannot be greater than 4.)

† There is an important incompatibility between standard subgrid modelling and the work of Lesieur & Schertzer. In the former the drain term is proportional to $k^2\epsilon^{\frac{1}{3}}E$, and ϵ itself decays with time: E_0 is then found to decay as $t^{-\frac{1}{2}}$ rather than as t^{-1} when $s = 1$. If the EDQNM closure is right, standard subgrid modelling needs substantial modification for small k. This correction will be more important for decaying quasi-homogeneous flows, which are eventually long-wave dominated, than for stationary inhomogeneous flows.

In evaluating (3.16) and (3.17) we have modified the energy $E(k)$ according to (3.36) and (3.37), but the inertial-range form (3.24) has been retained for $\eta(k)$. The response function could have been computed according to the EDQNM closure. The difference would probably have been small, since the denominators of (3.16) and (3.17) are dominated by the high-wavenumber contributions, which will be nearly of inertial-range form.

Figure 6 shows the effect of the spectrum (3.36) and (3.37) with $s = 1$ on the sharp filter. The non-dimensional net eddy viscosity

$$\nu_n^* = \nu_n / Ko\, D^{-1} \epsilon^{\frac{1}{3}} K_1^{-\frac{4}{3}} \tag{3.38}$$

is plotted as a function of $\lambda_1 = k/K_1$ for various values of K_1/K_p. When this ratio is large the spectrum is virtually of inertial-range form, and when it is $O(1)$ the peak of the production spectrum will be near the centre of the grid-scale range.

$$(k_{\text{peak}}/K_1 = 0{\cdot}5 \text{ when } K_1/K_p = 1{\cdot}651.)$$

As the peak of the production spectrum moves away from $k = 0$ and towards the cut, the pronounced cusp at $k = K_1$ is softened and reduced. Indeed $\nu_n(K_1)$ can be less than $\nu_n(0)$ for small K_1/K_p. For moderate values of this ratio, ν_n is nearly constant.

These calculations have been repeated for the Gaussian filter. The effect of the production spectrum is again to reduce ν_n but the change is much less than for the sharp filter.

3.2. *Anisotropy of the grid scales*

The results deduced above are ostensibly limited to (homogeneous) isotropic flows. This is very restrictive, and seems to make their relevance to large eddy simulations very doubtful. We shall now show that (with one fairly plausible assumption) the results are in fact independent of the symmetry of the grid scales, provided only that the subgrid scales are isotropic. This is much less restrictive, since as eddies become smaller they become increasingly isotropic.

We consider the drain term first. This may be written

$$S_{in}(\text{drain}; \mathbf{k}) = 2 \int_{-\infty}^{t} dt'' Q_{nc}(\mathbf{k}, t-t'') \times \iint \delta(\mathbf{k}-\mathbf{p}-\mathbf{r})\, d^3\mathbf{p}\, d^3\mathbf{r} P_{ijm}(\mathbf{k})\, G_{ja}^{(\text{res})}(\mathbf{p}, t-t'')\, P_{abc}(\mathbf{p})\, Q_{mb}(\mathbf{r}, t-t'') \tag{3.39}$$

[Leslie 1973, equation (4.35): we are working on the main time diagonal $t' = t$, and the first two terms on the right-hand side are identical]. $\mathbf{k}$ is a grid-scale wavenumber, while $\mathbf{p}$ and $\mathbf{r}$ are in the subgrid range. The functions $G_{ja}^{(\text{res})}(\mathbf{p}, t-t'')$ and $Q_{mb}(\mathbf{r}, t-t'')$ will therefore be isotropic. If the time dependences are exponential, the explicit forms are

$$\left.\begin{aligned} G_{ja}^{(\text{res})}(\mathbf{p}, t-t'') &= P_{ja}(\mathbf{p}) \exp\{-\eta(p)\,(t-t'')\}, \quad t > t'', \\ Q_{mb}(\mathbf{r}, t-t'') &= P_{mb}(\mathbf{r})\, q(r) \exp\{-\eta(r)\,|t-t''|\} \end{aligned}\right\} \tag{3.40}$$

[cf. (3.13)]. The grid-scale energy $Q_{nc}(\mathbf{k}, t-t'')$ is not assumed to be isotropic, and will not have this symmetry. However, we shall assume that it has the same form of time dependence, namely

$$Q_{nc}(\mathbf{k}, t-t'') = q_{nc}(\mathbf{k}) \exp\{-\eta(k)\,|t-t''|\}. \tag{3.41}$$

Equation (3.39) gives the whole of the inertial drain from wavenumber **k**. This can be divided into a grid-scale drain (which will be represented explicitly), Leonard and true subgrid terms. With the assumption (3.41) the true subgrid drain is

$$-2\xi_{ic}^{(d)}(\mathbf{k})\,\bar{q}_{cn}(\mathbf{k}), \tag{3.42}$$

where $\bar{q}_{cn}(\mathbf{k})$ is the grid-scale energy, and

$$\xi_{ic}^{(d)}(\mathbf{k}) = \iint \delta(\mathbf{k}-\mathbf{p}-\mathbf{r})\,d^3\mathbf{p}\,d^3\mathbf{r}\{1-G(p)\,G(r)\} \times P_{ijm}(\mathbf{k})\,P_{ja}(\mathbf{p})\,P_{abc}(\mathbf{p})\,P_{mb}(\mathbf{r})\,\frac{q(r)}{\eta(k)+\eta(p)+\eta(r)} \tag{3.43}$$

[cf. (3.10): the factor $G^2(k)$ has been absorbed into $\bar{q}$].

It is shown in the appendix that with the above assumptions

$$\xi_{ic}^{(d)}(\mathbf{k}) = P_{ic}(\mathbf{k})\,\nu_d(k) \tag{3.44}$$

[$\nu_d(k)$ being defined by (3.16)] and that it then follows that

$$(\text{true subgrid drain})_{in} = -2\nu_d(k)\,q_{in}(\mathbf{k}) \tag{3.45}$$

for any symmetry of $q_{in}(\mathbf{k})$.

The work of Herring (1974) shows that the assumption (3.41), on which this result appears to depend, is not particularly good. The time dependence of the anisotropic part of q_{cn} is rather different from that of the isotropic part, implying that the eddy viscosities for the two parts will differ. However the factor $\eta(k)$ in the denominator of (3.43), which specifies the time dependence of the grid scales, will be swamped by the subgrid time dependences $\eta(p)$ and $\eta(r)$. The implication is that the anisotropic and isotropic eddy viscosities will not differ much and that (3.45) is after all a good approximation.

In exactly the same way and at the same level of approximation, it may be shown that

$$(\text{true subgrid backscatter})_{in} = U(k)\,G_{in}^{(\text{res})}(\mathbf{k}, 0), \tag{3.46}$$

$U(k)$ being defined by (3.17), while $G_{in}^{(\text{res})}(\mathbf{k}, 0)$ specifies the symmetry of the response function at zero time separation. If we assume

$$G_{in}^{(\text{res})}(\mathbf{k}, 0) = q_{in}(\mathbf{k})/q(k), \tag{3.47}$$

which implies that the response function has the same symmetry as the correlation function, then the total drain and the backscatter may be rolled into a single net drain eddy viscosity according to (3.19) even when the flow is not isotropic.

However the work of Herring (1974; see also Schumann & Herring 1976) does not support (3.47) and this deduction from it. He finds that the response function is less anisotropic than the correlation function, and that the time dependence of the anisotropic part is of the form $t\exp[-\eta(k)\,t]$ rather than $\exp[-\eta(k)\,t]$: this reduces the anisotropic backscatter by a further factor

$$\eta(k)/[\eta(k)+\eta(p)+\eta(r)].$$

It might, therefore, be better to represent the backscatter as isotropic even when the grid-scale correlation tensor is not. There is, of course, no way of doing this while the subgrid effects are all rolled into a single net eddy viscosity.

We have not investigated the Leonard stress, but similar results can no doubt be proved for this term.

3.3. *Anisotropy of the subgrid scales*

Since the cut between the grid and subgrid scales will of necessity be at a comparatively low wavenumber, the subgrid scales may well be appreciably anisotropic. We have briefly examined the effect of an anisotropic subgrid component of the form generated by the action of a uniform velocity gradient on an isotropic field (Crow 1967, 1968; Leslie 1973, § 15.3). The results seem to be compatible with the treatment of this effect recommended by Schumann (1973), but the work is very heavy and has not been carried through to completion.

4. The magnitude of the eddy viscosity

The results of the previous section show that the error involved in treating the net eddy viscosity as constant is by no means unacceptable, if the filter is graded and/or the grid-scale spectrum is of production type. Once this approximation has been made, it remains only to determine the multiplying constant F of (2.12) by demanding that energy should be conserved. The calculation has been given above for a sharp filter and an inertial-range spectrum, and it will now be extended.

Energy balance requires

$$\int_0^\infty 2k^2\nu_n(av)\,\bar{E}(k)\,dk = \epsilon \tag{4.1}$$

and if the spectrum is of inertial-range type then

$$\bar{E}(k) = Ko\,\epsilon^{\frac{2}{3}}k^{-\frac{5}{3}}G^2(kh).$$

The dependence on the mesh spacing h is now shown explicitly, and the three filters all have width $2{\cdot}957/h$, which is the width of a top-hat filter on a mesh of spacing h (see § 2.2). It then follows that the constant F in (2.12) is given by

$$F = 1/(2Ko\,\beta_3), \tag{4.2}$$

where

$$\beta_3 = \int_0^\infty \xi^{\frac{1}{3}}\,G^2(\xi)\,d\xi. \tag{4.3}$$

Values of β_3 and F (with $Ko = 1{\cdot}5$) are given in table 1 below. Equation (3.13) is a special case of this result.

As noted in § 2, it is not easy to compute ϵ in a large eddy simulation and Smagorinsky (1963), whose lead has been followed by most later workers, represented ν_n by (2.13) rather than by (2.12). With this change ν_n is now a fluctuating quantity and the energy balance equation (4.1) must be modified to

$$\epsilon = 2c^2h^2 \oint k^2\langle \bar{S}^{\frac{1}{2}}\bar{u}_m\bar{u}_m\rangle(\mathbf{k})\,d^3\mathbf{k}. \tag{4.4}$$

It would be hard to evaluate the realization average $\langle \bar{S}^{\frac{1}{2}}\bar{u}\bar{u}\rangle$ properly, and Lilly (1966) therefore approximated it by

$$\langle \bar{S}^{\frac{1}{2}}\bar{u}\bar{u}\rangle \approx (\langle \bar{S}\rangle)^{\frac{1}{2}}\langle \bar{u}\bar{u}\rangle \tag{4.5}$$

since

$$\langle \bar{S}\rangle = 2\int_0^\infty k^2\bar{E}(k)\,dk = 2Ko\,\epsilon^{\frac{2}{3}}h^{-\frac{4}{3}}\beta_3 \tag{4.6}$$

	Filters		
	Top-hat	Gaussian	Sharp
β_3	3·373	3·375	3·183
F	0·0988	0·0988	0·105
c	0·176	0·176	0·184

TABLE 1. Eddy-viscosity constants for three filters.

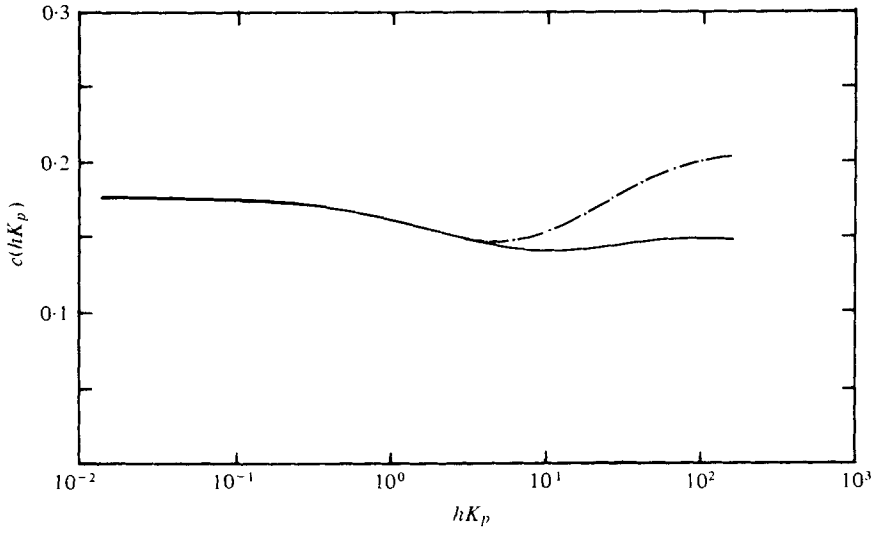

FIGURE 7. $c(hK_p)$ for the A_1 production spectrum. ——, top-hat filter; —·—, Gaussian filter.

is easily calculated. Substituting from (4.5) and (4.6) into (4.4), one derives Lilly's result

$$c = (2Ko\beta_3)^{-\frac{3}{4}} = F^{\frac{3}{4}}, \tag{4.7}$$

which is limited to an inertial-range spectrum. The approximation (4.5) introduces an error whose magnitude is very hard to assess, and this matter is discussed below.

Values of β_3, F and c for the top-hat, Gaussian and sharp filters are given in table 1. The constants for the top-hat and Gaussian filters are almost identical, and those for the sharp filter are not very different. This suggests that it is reasonable to regard filters of different shapes as equivalent if they have the same width.

Lilly has also calculated c for the top-hat filter, and found $c = 0{\cdot}185$ with $Ko = 1{\cdot}41$. Since c is proportional to $Ko^{-\frac{3}{4}}$, a change to the Ko value of 1·5 used throughout this paper would reduce Lilly's computed value of c to

$$0{\cdot}185 \times \left(\frac{1{\cdot}41}{1{\cdot}50}\right)^{\frac{3}{4}} = 0{\cdot}1766$$

in precise agreement with the value quoted in table 1 above. This is satisfactory, since it has not proved possible to relate Lilly's calculation in configuration space to the value deduced from (4.7). The relation of this result to the c values needed to stabilize actual large eddy simulations is considered later in this section.

Filter	σ
Sharp	1·370
Top-hat	0·489
Gaussian	0·340

TABLE 2. Values of the backscatter parameter σ.

The results in table 1 are valid when the grid-scale spectrum is of inertial-range form only, and (as noted in § 3.1.3) this will not be so in a 'real-life' large eddy simulation. We have therefore computed the dependence of c on hK_p for the Gaussian and top-hat filters, and the results are shown on figure 7.†

As a specific example of this work, the maximum of the A_1 spectrum is at

$$k/K_p = (3/5)^{\frac{3}{4}} = 0{\cdot}826$$

while the widths of all the filters are normalized to $W = 2{\cdot}957h^{-1}$. Thus for $hK_p = 1{\cdot}790$ the peak of the production spectrum is at $\frac{1}{2}W$, which is about where we should expect to find it in a well-conducted large eddy simulation. For this value of hK_p and the top-hat filter, $c = 0{\cdot}155$. For the same filter with a purely inertial-range spectrum, $c = 0{\cdot}176$ (see table 1), so that the change to a production-type spectrum does not have much effect on the value of the Lilly constant.

4.1. *Corrections to the global approach*

The global values of the net eddy viscosity ν_n quoted above have been computed by equating the net 'eddy–viscous' drain to the energy generation in the grid scales. (With a production-type spectrum, some of the generation will be in the subgrid scales.) The net drain is the difference between the gross outflow and the backscatter, and it turns out that the backscatter is larger than might have been guessed.

Its importance is conveniently measured by the parameter σ, defined by

$$\text{gross drain} = (1+\sigma)\,\epsilon_T, \quad \text{backscatter} = \sigma\epsilon_T, \tag{4.8}$$

ϵ_T (which may be less than ϵ) being the net drain. Values of σ for all three filters with an inertial-range spectrum are given in table 2. The value for the sharp filter is particularly striking, since it implies that the backscatter is greater than the net drain. If the inertial-range spectrum is replaced by the A_1 production-type spectrum, σ for the sharp filter decreases as hK_p is increased, passing through a minimum of 0·45 for $hK_p \approx 3{\cdot}3$. With the Gaussian filter and the A_1 spectrum, σ is virtually independent of hK_p if this parameter is less than 1·5; thereafter it rises slowly.

These large values of σ do not invalidate the c values quoted above provided that the flow is strictly homogeneous. They are a warning that inhomogeneity could easily produce an imbalance between the gross drain and the backscatter.

There is another effect which does produce a correction even in a homogeneous flow: this is the Leonard stress. As already noted, Lilly's formula (4.7) is derived by equating the eddy–viscous drain to the total generation. Modern practice is to use Lilly's

† The calculation is straightforward but tedious. The details have been suppressed to save space: they are available from the authors on request.

representation (2.13) for the true subgrid drain only: this is less than the total drain because of removal by the Leonard stress.

We have already noted that, for a Gaussian filter with an inertial-range spectrum, the Leonard stress removes 14·2% of the energy. The effect of this is to reduce c from 0·176 to 0·163.

4.2. *Evidence from numerical experiments*

At present it is customary to use the same c value over the whole of the flow field, and to adjust this single value empirically to produce agreement with the known time behaviour of the total energy. If the flow is stationary the criterion is simply that the energy should be constant. However a stationary flow must have real production terms, and these are essentially inhomogeneous. Deardorff (1970) and Schumann (1973, 1975) have studied fully developed channel flow, and they both find that a c value around 0·09 stabilizes the flow.

Closer examination shows that this apparent agreement is spurious. Deardorff uses a Smagorinsky-type subgrid model, and his c value is strictly comparable with that studied by Lilly and ourselves: his work does indeed imply that the theoretical values of c are too high by a factor of about two. Schumann's model is quite different: it is

$$\nu_n = c_2 h(\bar{E}')^{\frac{1}{2}}, \tag{4.9}$$

where $\bar{E}'$ is the subgrid energy [see (2.1)]. Schumann shows that for a sharp filter

$$c_2 = (hK_1)^{-1}(\tfrac{3}{2}Ko)^{-\frac{3}{2}} = 0{\cdot}100 \tag{4.10}$$

for $Ko = 1{\cdot}5$ and $hK_1 = 2{\cdot}957$ [see (2.22)]. (He puts $hK_1 = \pi$ and quotes a slightly different value of c_2.) For the same case

$$c = (hK_1)^{-1}(\tfrac{3}{2}Ko)^{-\frac{3}{4}} = 0{\cdot}184 \tag{4.11}$$

(see table 1), so that Deardorff's constant c should be nearly twice as large as Schumann's constant c_2.

Schumann finds that the theoretical value of c_2 is not grossly wrong, and the incompatibility between this and Deardorff's finding cannot be resolved with the available information.†

Since it contains no production a homogeneous flow must decay and c must be adjusted so that the simulation reproduces an experimental decay rate. Grid turbulence is generally reckoned to be nearly homogeneous in the centre of the wind tunnel, the time decay being mimicked by the mean-flow convection of the turbulence away from the grid. Kwak *et al.* (1975) have made a homogeneous large eddy simulation of the grid-turbulence measurements of Comte-Bellot & Corrsin (1971). They find that with a c-value of 0·206 the calculation matches the experimental energy decay rate. This is quite close to Lilly's value (0·185).‡ The agreement seems to be fortuitous because of the following:

(i) The unknown error in Lilly's approximation (4.5).

(ii) The effect of Leonard stresses, which were ignored by Lilly but were included in the Kwak *et al.* simulation and which, as noted above, will reduce the value of c.

(iii) The inhomogeneity of the actual flow.

† Deardorff (1971) suggests that the disagreement may be due to the effect of shear, which is not included in Lilly's analysis.

‡ Kwak *et al.* say that their value agrees with Lilly's: this seems to be wrong.

(iv) The error in the standard subgrid model of the long waves (see footnote in § 3.1.3): these will eventually dominate the decay.

Clearly there is a good deal more to be done, even in this simplest example of the use of subgrid modelling.

5. Implications for large eddy simulation

Implicit in § 4.2 is the assumption that ν_n values deduced for a closed calculation can be applied without change to a large eddy simulation. We shall now discuss the validity of this application. We do not consider the effect of the unknown errors in the classical closures.

5.1. *The validity of unaveraging*

When the results of a closed calculation are used in this way one is effectively 'unaveraging' the grid scales while leaving the subgrid scales averaged. It is natural to ask whether this can be valid, and whether the simulation will not be affected by quantities with zero mean which were destroyed by the averaging process and which are not recreated by the crude unaveraging used above. One could have more confidence in the process if the grid and subgrid scales were well separated, but they are not. They are adjacent if the filter is sharp, and they actually overlap if it is graded.

The simple answer is that the difficulty lies as much in the crudeness of the subgrid model as in the unaveraging process. With Smagorinsky's simple model (2.13) we can demand no more than that the mean energy should be conserved at each point. Apart from any defects in the classical closures and the technical errors listed in § 4.2 (the latter being remediable, at least in principle) the method of this paper does just this, and no more can be accommodated within the standard framework.

Since so much has been thrown away, any individual realization of the large eddy simulation must be in error. However, averages deduced from it should be much less wrong, and it is usually these averages which are wanted. Large eddy simulation is normally used, not because it can furnish information on fluctuating quantities, but because it is an effective way of computing averages.

Rose (1977) has applied renormalization group methods to subgrid modelling and in this way has been able to avoid averaging the grid scales. He shows that there is a hierarchy of effects, of which the first three are gross drain, which is of eddy-viscosity form, backscatter and eddy-mediated advection. The first two transfer energy in the mean, the higher terms do not.

At present not even the backscatter is represented explicitly: it is merely allowed to modify the eddy viscosity. The first forward step is obviously to include the backscatter, and we have shown that the necessary information can be obtained from the classical closures. We have also shown that the backscatter is large, and that it is likely to be more isotropic than the gross drain or outflow. It therefore seems well worthwhile to test the effect of representing it explicitly.

The effect of unaveraging the Lilly approximation (4.5) is to replace Smagorinsky's subgrid model (2.13) by

$$\nu_e = c^2 h^2 \langle \bar{S} \rangle^{\frac{1}{2}}. \tag{5.1}$$

The realization average can be implemented either as an average over a volume surrounding the point in question, or as an integral over past time. Love (1977,

private communication) has tested this modification on Burgers' equation (using volume averaging) and has found that it improves the modelling. It would be interesting to try it on the Navier–Stokes equation.

5.2. *The effect of finite subgrid time scale*

In § 3.1 we limited ourselves to the main time diagonal $t = t'$, and we integrated out the time dependence of the inertial transfer term with the help of the assumption (3.13). According to Kraichnan's original (or Eulerian) direct-interaction approximation, the forward scatter or drain part of this term has the detailed time structure

$$\overset{\Delta}{\sum}\int dt'' G^{(\mathrm{res})}(\mathbf{p}, t-t'')\, Q(\mathbf{r}, t-t'')\, Q(\mathbf{k}, t''-t').$$

This can be generated by adding to the primitive or unaveraged Navier–Stokes equations a drain term

$$\int_{-\infty}^{t} \zeta(\mathbf{k}, t-t'')\, u(t'')\, dt'', \tag{5.2}$$

where

$$\zeta(\mathbf{k}, t-t'') = \overset{\Delta}{\sum} G^{(\mathrm{res})}(\mathbf{p}, t-t'')\, Q(\mathbf{r}, t-t''). \tag{5.3}$$

If we assume that the subgrid fluctuations are much faster than those of the grid scales, then

$$(5.2) \to \nu_d k^2 u \quad \text{with} \quad \nu_d k^2 = \int_{-\infty}^{t} \zeta(\mathbf{k}, t-t'')\, dt''. \tag{5.4}$$

The representation (5.2) is presumably more faithful than (5.4), in that it should enable the large eddy simulation to follow the detailed fluctuations.

The effect of this can be tested relatively easily, once the net drain has been separated into gross drain and backscatter, though the structure of ζ may lead to storage problems.

5.3. *The effect of inhomogeneity*

In this application, their inability to say anything practically useful about the effects of inhomogeneity is the Achilles heel of the classical closures. (Their inability to represent intermittency is much more fundamental, but its practical consequences may well be much smaller.)

The results deduced above can be valid only if the subgrid scales and the smallest grid scales are nearly homogeneous. It seems likely that, if this condition is satisfied, the inhomogeneity of the largest scales (which is inevitable in any simulation of a real flow) will not invalidate the results; however this still remains to be proved.

It is possible to make scales of the order of the grid spacing reasonably homogeneous except near boundaries, though this condition is often violated to save machine time. Thus the results of this paper should be applicable away from the boundaries, provided enough mesh points are used. In particular it would, in our opinion, be valid to allow Smagorinsky's constant c to vary across the flow field as a function of hK_p (see § 3.1.3 and figure 6), and a method has been worked out for determining this quantity in a practical calculation.† However c does not depend strongly on hK_p, and the difference between representing this variation and using a constant value of c would probably be rather small.

† Details are available from the authors on request.

The theory presented above is invalid in the grid volumes adjoining boundaries, because of strong inhomogeneity and the absence of an inertial range in the inner parts of these regions. The boundary conditions used in existing simulations are heuristic (e.g. Schumann 1973, 1975) and this is probably the weakest part of the theory of large eddy simulation.

6. Conclusions and recommendations

(i) We have confirmed Kraichnan's (1976) result that effective eddy viscosities can be deduced from the classical closures. Kraichnan found that the effective eddy viscosity varies strongly with k, but this result is now seen to be peculiar to the combination of an inertial-range grid-scale spectrum with a sharp filter. With more realistic spectra and filters, it is reasonably constant.

(ii) Smagorinsky (1963) estimated ϵ from the grid-scale strain function $\bar{S}^{\frac{1}{2}}$. The classical closures suggest that this estimator should be replaced by $\langle \bar{S} \rangle^{\frac{1}{2}}$ or by a volume average. This works well for Burgers' equation, and should be tried for the Navier–Stokes equations.

(iii) The results are deduced for an isotropic flow. It has been demonstrated that they are valid whatever the symmetry of the grid scales, provided only that the subgrid scales are isotropic. It has been confirmed that there is no special difficulty in extending the work to anisotropic subgrid scales.

(iv) The analysis has revealed a number of weaknesses in the conventional subgrid model, even when the flow is isotropic. In particular, the recent paper of Lesieur & Schertzer (1977) suggests that the model is seriously in error for the long waves. Our work also suggests that it would be advantageous to model the gross drain and the backscatter separately, and that the finite subgrid time scale could then be allowed for explicitly by way of a time-dependent eddy viscosity.

(v) We have separated the Leonard term from the 'true' subgrid stress, and find that in a typical case this term accounts for 14% of the total drain. Leonard's approximate representation overestimates the Leonard drain, but the consequent error in the subgrid drain amounts to a few per cent only.

(vi) The results are formally valid for homogeneous flows only, and there is at present no way of extending them to real, inhomogeneous flows. Though we have no proof we think it likely that they are valid for the interior regions of such flows, provided that eddies comparable in size with the mesh spacing are reasonably homogeneous. The flow in mesh volumes adjoining boundaries is necessarily inhomogeneous, and the boundary conditions should correct empirically any deficiency in the subgrid model in these regions.

We are grateful to Dr J. R. Herring, Dr R. H. Kraichnan and Dr H. A. Rose for helpful discussions and correspondence and to Dr Kraichnan for comments which have helped us to improve the presentation. Turbulence research in the Department of Nuclear Engineering at Queen Mary College is supported by the Science Research Council, and Dr G. L. Quarini is indebted to the Council for a (predoctoral) Research Studentship.

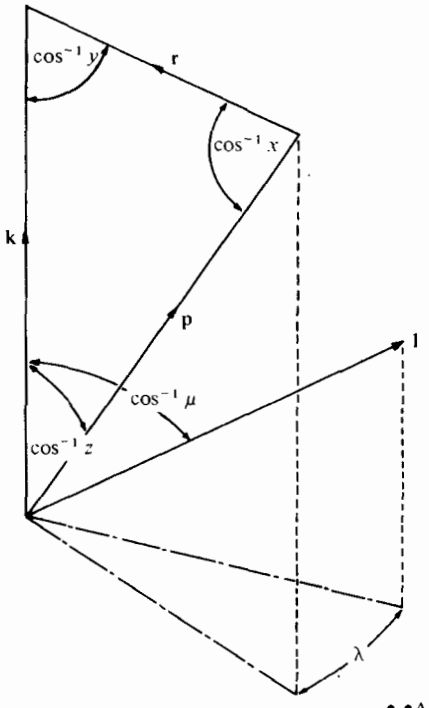

FIGURE 8. Illustration of the operation $\iint^{\Delta} d^3p\, d^3r$.

Appendix. Evaluation of the generalized eddy viscosity

This quantity is defined by (3.43). The integral operator

$$\overset{\Delta}{\Sigma} = \iint \delta(\mathbf{k}-\mathbf{p}-\mathbf{r})\, d^3\mathbf{p}\, d^3\mathbf{r}$$

is equivalent to

$$\iint \frac{pr}{k}\, dp\, dr \oint d\lambda \tag{A 1}$$

(Leslie 1973). As indicated in figure 8, the integration over the angular variable λ is carried out by rotating the **p** and **r** vectors round **k** while the shape and size of the triangle **k**, **p**, **r** is held fixed. If the integrand is a function of the scalars k, p and r only, then this operation simply multiplies that integrand by 2π. If however the integrand depends on the vectors **k**, **p** and **r**, then the effect of the rotation is to remove the dependence on the angle variables Ω_p and Ω_r: the integral may still depend on the vector **k**, but it will be a function of the scalars p and r only. The integration over these variables is then limited to the region

$$|k-p| < r < k+p, \tag{A 2}$$

in which **p** and **r** can form a triangle with **k**.

Equation (3.43) of the main text may therefore be rewritten

$$\xi_{ic}^{(d)}(\mathbf{k}) = \iint^{\Delta} \frac{pr}{k}\, dp\, dr\, \frac{q(r)}{\eta(k)+\eta(p)+\eta(r)}\, C_{ic}(\mathbf{k},p,r), \tag{A 3}$$

where
$$C_{ic}(\mathbf{k}, p, r) = \oint d\lambda B_{ic}(\mathbf{k}, \mathbf{p}, \mathbf{r}) \tag{A 4}$$

and
$$B_{ic}(\mathbf{k}, \mathbf{p}, \mathbf{r}) = P_{ijm}(\mathbf{k}) P_{jbc}(\mathbf{p}) P_{mb}(\mathbf{r}) \tag{A 5}$$

since $P_{ja}(\mathbf{p}) P_{abc}(\mathbf{p}) = P_{jbc}(\mathbf{p})$. Now $B_{cc}(\mathbf{k}, \mathbf{p}, \mathbf{r})$ is a function of the scalars k, p and r equal to
$$J_3(k, p, r) = 2k^2 b(k, p, r), \tag{A 6}$$

where
$$b(k, p, r) = (p/k)(xy + z^3) \tag{A 7}$$

is the quantity which first appears in (3.14).

To prove (A 6) and (A 7) Leslie (1973, appendix) divides $J_3 = B_{cc}(k, p, r)$ into four parts [his equation (A 16)]. We make the same division of B_{ic}:
$$B_{ic}(\mathbf{k}, \mathbf{p}, \mathbf{r}) = \sum_{n=1}^{4} B_{ic}^{(n)}(\mathbf{k}, \mathbf{p}, \mathbf{r}). \tag{A 8}$$

For instance
$$\begin{aligned} B_{ic}^{(2)} &= k_m P_{mb}(\mathbf{r}) p_b \times P_{ij}(\mathbf{k}) P_{jc}(\mathbf{p}) \\ &= kp(z + xy) \,.\, P_{ij}(\mathbf{k}) P_{jc}(\mathbf{p}) \end{aligned} \tag{A 9}$$

and the definition of the other three terms will be obvious by comparison with Leslie's equation (A 17).

The contribution of this term to C_{ic} is
$$C_{ic}^{(2)}(\mathbf{k}, p, r) = kp(z + xy) \oint P_{ij}(\mathbf{k}) P_{jc}(\mathbf{p}) \, d\lambda. \tag{A 10}$$

To evaluate the inner integral we use a Cartesian co-ordinate system with the 1 direction parallel to $\mathbf{k}$. In this system
$$P_{ij}(\mathbf{k}) = \delta_{2i}\delta_{2j} + \delta_{3i}\delta_{3j} \tag{A 11}$$

and
$$P_{ij}(\mathbf{k}) P_{jc}(\mathbf{p}) = \delta_{2i}\left(\delta_{2c} - \frac{p_2 p_c}{p^2}\right) + \delta_{3i}\left(\delta_{3c} - \frac{p_3 p_c}{p^2}\right). \tag{A 12}$$

Referring to figure 8, the components of $\mathbf{p}$ are
$$(p_1, p_\perp \cos\lambda, p_\perp \sin\lambda), \tag{A 13}$$

where $p_1 = zp$, while
$$p_\perp = (p^2 - p_1^2)^{\frac{1}{2}} = p(1 - z^2)^{\frac{1}{2}} \tag{A 14}$$

is the component perpendicular to $\mathbf{k}$. After integration only the terms $c = 2, 3$ survive in $p_2 p_c / p^2$ and $p_3 p_c / p^2$ respectively. Thus
$$\begin{aligned} \oint d\lambda P_{ij}(\mathbf{k}) P_{jc}(\mathbf{p}) &= 2\pi (\delta_{2i}\delta_{2c} + \delta_{3i}\delta_{3c}) \left(1 - \frac{1}{2}\frac{p_\perp^2}{p^2}\right) \\ &= \pi(1 + z^2) P_{ic}(\mathbf{k}), \end{aligned} \tag{A 15}$$

so that
$$\begin{aligned} C_{ic}^{(2)}(\mathbf{k}, p, r) &= \pi P_{ic}(\mathbf{k}) kp(1 + z^2)(z + xy) \\ &= \pi P_{ic}(\mathbf{k}) B_2(k, p, r), \end{aligned}$$

B_2 being the quantity defined by Leslie [1973, equation (A 18)].

With rather more labour it may be shown that the same result holds for the other three components, so that
$$C_{ic}(\mathbf{k}, p, r) = \pi P_{ic}(\mathbf{k}) J_3(k, p, r). \tag{A 16}$$

Substituting from (A 16), (A 6) and (A 7) into (A 3), we confirm equation (3.44) of the main text [cf. (3.16)]. Now

$$q_{cn}(\mathbf{k}) = \langle \tilde{u}_c(\mathbf{k}, t)\, \tilde{u}_n(-\mathbf{k}, t) \rangle$$

and since u_c satisfies the continuity condition $k_c \tilde{u}_c(\mathbf{k}) = 0$, q_{cn} must be of the form

$$q_{cn}(\mathbf{k}) = P_{ce}(\mathbf{k})\, \hat{q}_{ef}(\mathbf{k})\, P_{fn}(\mathbf{k}),$$

where $\hat{q}_{ef}$ may have any symmetry. Since $P_{ic}(\mathbf{k})\, P_{ce}(\mathbf{k}) = P_{ie}(\mathbf{k})$ equation (3.45) of the main text follows at once.

If we assume

$$G_{in}^{(\mathrm{res})}(\mathbf{k}, \tau) = G_{in}^{(\mathrm{res})}(\mathbf{k}, 0) \exp[-\eta(k) . \tau] \tag{A 17}$$

then the result

$$(\text{true subgrid backscatter})_{in} = U(k)\, P_{ic}(\mathbf{k})\, G_{cn}^{(\mathrm{res})}(\mathbf{k}, 0) \tag{A 18}$$

may be derived by the methods used above: the evaluation of further factors similar to C_{ic} [see (A 4)] can be avoided by using a relation analogous to equation (A 28) of Leslie (1973). Equation (3.46) of the main text now follows from (A 18) by continuity.

REFERENCES

Comte-Bellot, G. & Corrsin, S. 1971 Simple Eulerian time correlation of full- and narrow-band velocity signals in grid-generated 'isotropic' turbulence. *J. Fluid Mech.* **48**, 273.

Corrsin, S. 1961 Turbulent flow. *Amer. Scientist* **49**, 300.

Crow, S. C. 1967 Visco-elastic character of fine-grained isotropic turbulence. *Phys. Fluids* **10**, 1587.

Crow, S. C. 1968 Visco-elastic properties of fine-grained incompressible turbulence. *J. Fluid Mech.* **33**, 1.

Deardorff, J. W. 1970 A numerical study of three-dimensional turbulent channel flow at large Reynolds numbers. *J. Fluid Mech.* **41**, 453.

Deardorff, J. W. 1971 On the magnitude of the subgrid scale eddy coefficient. *J. Comp. Phys.* **7**, 120.

Herring, J. R. 1974 Approach of axisymmetric turbulence to isotropy. *Phys. Fluids* **17**, 859.

Kraichnan, R. H. 1964 Direct interaction approximation for shear and thermally driven turbulence. *Phys. Fluids* **7**, 1048.

Kraichnan, R. H. 1971 An almost-Markovian Galilean-invariant turbulence model. *J. Fluid Mech.* **47**, 513.

Kraichnan, R. H. 1976 Eddy viscosity in two and three dimensions. *J. Atmos. Sci.* **33**, 1521.

Kwak, D., Reynolds, W. C. & Ferziger, J. H. 1975 Three-dimensional time dependent computation of turbulent flow. *Stanford Univ. Rep. TF-5.*

Leonard, A. 1974 Energy cascade in large-eddy simulations of turbulent fluid flows. *Adv. in Geophys.* A **18**, 237.

Lesieur, M. & Schertzer, D. 1977 Amortissement autosimilaire d'une turbulence a grand nombre de Reynolds. *J. Méc.* **17**, 609.

Leslie, D. C. 1973 *Developments in the Theory of Turbulence.* Oxford: Clarendon Press.

Lilly, D. K. 1966 On the application of the eddy viscosity concept in the inertial sub-range of turbulence. *N.C.A.R. Rep.* no. 123.

Lilly, D. K. 1967 The representation of small-scale turbulence in numerical simulation experiments. *Proc. I.B.M. Sci. Comp. Symp. on Environ. Sci.* p. 1866 (publ. 1967).

Monin, A. S. & Yaglom, A. M. 1975 *Statistical Fluid Mechanics*, English edn. M.I.T. Press.

Orszag, S. A. 1970 Analytical theories of turbulence. *J. Fluid Mech.* **41**, 363.

Orszag, S. A. & Patterson, G. S. 1972 Numerical simulation of three-dimensional homogeneous isotropic turbulence. *Phys. Rev. Lett.* **28**, 76.

ROSE, H. 1977 Eddy diffusivity, eddy noise and subgrid-scale modelling. *J. Fluid Mech.* **81**, 719.

SCHUMANN, U. 1973 Ein Verfahren zur direkten numerischen Simulation turbulenter Strömungen in Platten- und Ringspaltkanalen und über seine Anwendung zur Intersuchung von Turbulenzmodellen. Ph.D. thesis, Karlsruhe University. (Available as *Rep.* KFK 1854.)

SCHUMANN, U. 1975 Subgrid scale model for finite difference simulations of turbulent flows in plane channels and annuli. *J. Comp. Phys.* **18**, 376.

SCHUMANN, U. & HERRING, J. R. 1976 Axisymmetric homogeneous turbulence: a comparison of direct spectral simulations with the direct-interaction approximation. *J. Fluid Mech.* **76**, 755.

SMAGORINSKY, J. S. 1963 General circulation experiments with the primitive equations. I: the basic experiment. *Mon. Weath. Rev.* **91**, 99.